Lecture Notes on Topological Insulators

Anouar Moustaj

FTCM 2024

Transcription Status

This file is a written LaTeX reconstruction of the handwritten PDF `Lectures_TI.pdf` using LLMs. The aim is to preserve all mathematical and conceptual material from the notes. Equations or handwritten fragments that could not be unambiguously read are not omitted; they are marked explicitly with `\transcriptiontodo{...}`. The schematic figures in these notes are redrawn in TikZ rather than embedded as scans of the handwritten pages.

Reference Material

[Source handwritten page 1]

- Bradlyn, SciPost Lecture Notes **51** (2022).
- Sergeev, SciPost Lecture Notes **67** (2023).
- J. K. Asboth, L. Oroszlany, and A. Palyi, *A Short Course on Topological Insulators*, Lecture Notes in Physics, Springer (2016), arXiv:1509.02295.
- B. A. Bernevig and T. L. Hughes, *Topological Insulators and Topological Superconductors*, Princeton University Press (2013).

Contents

1 Lecture 1: Adiabatic Transport and Geometric Phase

1.1 Ingredients

[Source handwritten page 2]

Let M be a smooth manifold. The parameters of the Hamiltonian live on this manifold and are denoted by $\boldsymbol{x} \in M$.

We consider a family of Hamiltonians depending smoothly on $\boldsymbol{x}$,

$$H(\boldsymbol{x}). \tag{1}$$

At every $\boldsymbol{x}$, the Hamiltonian has a discrete spectrum:

$$H(\boldsymbol{x}) \left|n(\boldsymbol{x})\right\rangle = E_n(\boldsymbol{x}) \left|n(\boldsymbol{x})\right\rangle . \tag{2}$$

The vector space spanned by a chosen set of states is the relevant band subspace. We want to focus on a subspace

$$\mathcal{R}(\boldsymbol{x}) = \text{span}\{|n(\boldsymbol{x})\rangle\}_{n=1}^{N}. \tag{3}$$

The essential assumption is that this collection of bands is separated from the rest of the spectrum by a gap. Schematically, if

$$H(\boldsymbol{x}) \left|n(\boldsymbol{x})\right\rangle = E_n(\boldsymbol{x}) \left|n(\boldsymbol{x})\right\rangle , \tag{4}$$

then the chosen energies $E_n(\boldsymbol{x})$ remain isolated from the complementary energies by a finite gap Δ.

Transcription needed: The handwritten inequality specifying the separation between the relevant subspace $\mathcal{R}(\boldsymbol{x})$ and the rest of the spectrum is partially illegible in the scan. It appears to state a finite minimum gap condition, $\min |E_i - E_j| \geq \Delta$, for states inside versus outside the chosen band subspace.

We can work entirely inside this subspace by defining the projection operator

$$P(\boldsymbol{x}) = \sum_{n=1}^{N} \left|n(\boldsymbol{x})\right\rangle \left\langle n(\boldsymbol{x})\right| . \tag{5}$$

Projectors allow a simple geometric formulation of the adiabatic theorem.

1.2 Adiabatic Theorem

[Source handwritten page 3]

Statement. A physical system remains in its instantaneous eigenstate if a perturbation acts slowly enough and if there is a gap between the eigenvalue and the rest of the Hamiltonian spectrum.

In simple words: if the system begins close to an eigenstate, it remains close to the corresponding instantaneous eigenstate under sufficiently slow evolution.

Let $U(t)$ be the exact time-evolution operator and $U_a(t)$ the adiabatic evolution operator. The adiabatic evolution satisfies the intertwining relation

$$U_a(t)P(0) = P(t)U_a(t), \tag{6}$$

where $P(t) = P(\boldsymbol{x}(t))$.

A quantitative statement in the notes is the adiabatic approximation

$$\|U(t)P(0) - U_a(t)P(0)\| \longrightarrow 0 \qquad \text{as} \qquad T \to \infty, \tag{7}$$

where T is the total time of adiabatic evolution. The limit $T \to \infty$ is the adiabatic limit.

Transcription needed: The handwritten line labelled "Garnutt" is likely a reference to a rigorous norm estimate for the adiabatic theorem. The exact name/source and bound are unclear.

The handwritten notes refer to a proof in lecture notes by Prof. Miles Stoudenmire, University of Waterloo. The next goal is to derive an expression for $U_a(t)$.

1.3 Geometric Evolution

[Source handwritten page 4]

The defining relation for adiabatic transport is

$$P(t)U_a(t) = U_a(t)P(0). \tag{8}$$

Equivalently,

$$U_a^\dagger(t)P(t)U_a(t) = P(0). \tag{9}$$

Differentiating gives a condition on the generator of U_a.

Let U_a satisfy

$$\frac{\mathrm{d}U_a}{\mathrm{d}t} = K(t)U_a(t). \tag{10}$$

The notes state that this is satisfied by

$$K(t) = [\dot{P}(t), P(t)]. \tag{11}$$

The suggested verification uses the projector identity

$$P^2 = P. \tag{12}$$

Differentiating $P^2 = P$ gives

$$\dot{P}P + P\dot{P} = \dot{P}, \tag{13}$$

and multiplying by P on both sides yields

$$P\dot{P}P = 0. \tag{14}$$

Therefore the differential equation is

$$\frac{\mathrm{d}U_a}{\mathrm{d}t} = [\dot{P}(t), P(t)]U_a(t), \tag{15}$$

with solution

$$U_a(t) = \mathcal{T} \exp\left[\int_0^t [\dot{P}(t'), P(t')]\,\mathrm{d}t'\right]. \tag{16}$$

Using a parametrized path $\boldsymbol{x} = \boldsymbol{x}(t)$ in parameter space, one may write

$$\dot{P} = \dot{x}^\mu \partial_\mu P, \tag{17}$$

and therefore the evolution is a path-ordered exponential along the path $\gamma : t \mapsto \boldsymbol{x}(t)$:

$$U_a[\gamma] = \mathcal{P} \exp \int_\gamma [\mathrm{d}P, P]. \tag{18}$$

Transcription needed: The handwritten page contains a formula involving $W_a = \mathcal{P} \exp(\int P \, \mathrm{d}P \, P)$ or a closely related object. The exact operator ordering is unclear. The projector expression above is the standard Kato adiabatic evolution.

1.4 Geometric Action on States

[Source handwritten page 5]

Question: how does the state behave as it moves through the manifold?

Let

$$|\psi(t)\rangle = U_a(t) \, |\psi(0)\rangle \, . \tag{19}$$

If the initial state lies in the initial subspace,

$$P(0) \, |\psi(0)\rangle = |\psi(0)\rangle \, , \tag{20}$$

then, using the intertwining relation,

$$P(t) \, |\psi(t)\rangle = P(t) U_a(t) \, |\psi(0)\rangle = U_a(t) P(0) \, |\psi(0)\rangle = |\psi(t)\rangle \, . \tag{21}$$

Thus states in the subspace $\mathcal{R}(\boldsymbol{x})$ stay in that subspace.

The notes then use $P\dot{P}P = 0$ to obtain the condition of parallel transport:

$$P(t) \frac{\mathrm{d}}{\mathrm{d}t} \, |\psi(t)\rangle = 0. \tag{22}$$

This says that the component of the time derivative inside the instantaneous subspace vanishes. Geometrically, this defines a connection on the vector bundle of occupied states.

The object $A(t)$ appearing in this parallel-transport equation is the Berry connection on a fiber bundle.

1.5 Fiber-Bundle Language

[Source handwritten page 6]

The notes describe the bundle language in the simple $U(1)$ case and then indicate the non-Abelian $U(N)$ generalization.

A G-bundle is a collection of spaces organized as

$$E \xrightarrow{\pi} M, \tag{23}$$

with fiber F and structure group G. A principal bundle has fiber $F = G$.

Here the fiber over $\boldsymbol{x}$ is the vector space of states at $\boldsymbol{x}$. At each point $\boldsymbol{x} \in M$ there is a local $U(1)$ invariance,

$$|u(\boldsymbol{x})\rangle \sim \mathrm{e}^{\mathrm{i}\phi(\boldsymbol{x})} \, |u(\boldsymbol{x})\rangle \, . \tag{24}$$

Thus in the one-band case we have a $U(1)$ bundle. The physical states are equivalence classes under local phase rotations.

A projection map sends states in the total space to points in the base manifold:

$$\pi : |u(\boldsymbol{x})\rangle \mapsto \boldsymbol{x}. \tag{25}$$

A gauge fixing corresponds to choosing a section

$$s : M \to E, \tag{26}$$

such that

$$\pi \circ s = \mathrm{id}_M \,. \tag{27}$$

The Berry connection is then

$$A = \mathrm{i} \,\langle u(\boldsymbol{x}) \,|\, \mathrm{d}u(\boldsymbol{x})\rangle = A_\mu(\boldsymbol{x})\, \mathrm{d}x^\mu. \tag{28}$$

The Berry curvature, or field strength, is

$$F = \mathrm{d}A. \tag{29}$$

In components,

$$F_{\mu\nu} = \partial_\mu A_\nu - \partial_\nu A_\mu. \tag{30}$$

Under a gauge transformation,

$$A \mapsto A - \mathrm{d}\phi, \tag{31}$$

but

$$F \mapsto F. \tag{32}$$

The curvature is gauge invariant and is central for topological insulators.

In general, for N occupied states, the gauge group becomes $U(N)$ and the connection is non-Abelian:

$$A_{mn} = \mathrm{i} \,\langle u_m \,|\, \mathrm{d}u_n\rangle \,, \tag{33}$$

with curvature

$$F = \mathrm{d}A - \mathrm{i}A \wedge A \tag{34}$$

up to convention. Some communities write $F = \mathrm{d}A + A \wedge A$ depending on whether the connection includes a factor of i.

1.6 Example: Spin in a Slowly Varying Magnetic Field

[Source handwritten page 7]

Consider

$$H(\boldsymbol{B}) = \mu\, \boldsymbol{B} \cdot \boldsymbol{\sigma}, \tag{35}$$

with a magnetic field of constant magnitude,

$$\boldsymbol{B} = B \begin{pmatrix} \cos\phi \sin\theta \\ \sin\phi \sin\theta \\ \cos\theta \end{pmatrix} = B\hat{\boldsymbol{n}}. \tag{36}$$

The adiabatic evolution has two bands that do not cross as long as $B \neq 0$. For the lower band, the projector is

$$P = \frac{1}{2}\left(\mathbb{1} - \hat{\boldsymbol{n}} \cdot \boldsymbol{\sigma}\right). \tag{37}$$

The Berry connection can be computed from the projector expression. The notes indicate the object

$$[\dot{P}, P] = \frac{\mathrm{i}}{2}\left(\hat{\boldsymbol{n}} \times \dot{\hat{\boldsymbol{n}}}\right) \cdot \boldsymbol{\sigma}, \tag{38}$$

or equivalently in components,

$$K = [\dot{P}, P] = \frac{\mathrm{i}}{2}\epsilon_{ijk}\hat{n}_i\dot{\hat{n}}_j\sigma_k. \tag{39}$$

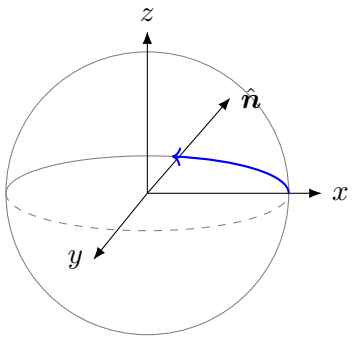

Slow motion of $\hat{\boldsymbol{n}}$ on the sphere

Figure 1: Schematic parameter sphere for the spin example.

[Source handwritten page 8]

For evolution along the equator, take

$$\theta = \frac{\pi}{2}, \qquad \phi = \omega t. \tag{40}$$

Then

$$\hat{\boldsymbol{n}}(t) = (\cos\omega t, \sin\omega t, 0), \tag{41}$$

and

$$\hat{\boldsymbol{n}} \times \dot{\hat{\boldsymbol{n}}} = (0, 0, \omega). \tag{42}$$

Thus the geometric generator is proportional to σ_z:

$$K = \frac{\mathrm{i}\omega}{2}\sigma_z. \tag{43}$$

The adiabatic geometric evolution is therefore

$$U_a(t) = \exp\left(\frac{\mathrm{i}\omega t}{2}\sigma_z\right) = \begin{pmatrix} \mathrm{e}^{\mathrm{i}\omega t/2} & 0 \\ 0 & \mathrm{e}^{-\mathrm{i}\omega t/2} \end{pmatrix}. \tag{44}$$

The notes write a trigonometric form,

$$U_a(t) = \cos\left(\frac{\omega t}{2}\right)\mathbb{1} + \mathrm{i}\sin\left(\frac{\omega t}{2}\right)\sigma_z, \tag{45}$$

up to sign conventions.

For a closed loop around the equator, $t = 2\pi/\omega$, so

$$U_a(2\pi/\omega) = -\mathbb{1}. \tag{46}$$

The state acquires a phase of π after a closed-loop evolution:

$$|\psi(0)\rangle \mapsto -|\psi(0)\rangle\,. \tag{47}$$

Transcription needed: The exact initial spinor and evolved spinor written in the handwritten notes are partly OCR-corrupted. The intended result is that a lower band spinor transported around the equator acquires the Berry phase π.

1.7 Using a Basis

[Source handwritten page 9]

The projector formulation is geometric, but for calculations we usually choose a basis in the occupied subspace. Let

$$P(\boldsymbol{x}) = \sum_{n=1}^{N} |u_n(\boldsymbol{x})\rangle\,\langle u_n(\boldsymbol{x})|\,. \tag{48}$$

Write a state in the subspace as

$$|\psi(\boldsymbol{x})\rangle = \sum_n a_n(\boldsymbol{x})\,|u_n(\boldsymbol{x})\rangle\,. \tag{49}$$

Parallel transport imposes

$$P\,\mathrm{d}\,|\psi\rangle = 0. \tag{50}$$

This gives

$$\mathrm{d}a_m + \sum_n \langle u_m\,|\,\mathrm{d}u_n\rangle\,a_n = 0. \tag{51}$$

Defining the Berry connection in a basis by

$$A_{mn}(\boldsymbol{x}) = \mathrm{i}\,\langle u_m(\boldsymbol{x})\,|\,\mathrm{d}u_n(\boldsymbol{x})\rangle\,, \tag{52}$$

the coefficients obey

$$\mathrm{d}a_m - \mathrm{i}\sum_n A_{mn}a_n = 0. \tag{53}$$

The solution is a Wilson line:

$$a_m(\boldsymbol{x}) = \sum_n \left[\mathcal{P}\exp\left(\mathrm{i}\int_\gamma A\right)\right]_{mn} a_n(\boldsymbol{x}_0). \tag{54}$$

The Wilson-line matrix is

$$W_{mn} = \langle u_m(\boldsymbol{x})\,|\,U_a(\gamma)u_n(\boldsymbol{x}_0)\rangle\,. \tag{55}$$

For a closed path, W is a holonomy.

The notes emphasize that for a closed path the spectrum of W is gauge invariant. Under a $U(N)$ gauge transformation

$$|u_n\rangle \mapsto \sum_m |u_m\rangle\,S_{mn}, \tag{56}$$

the Wilson loop transforms as

$$W \mapsto S^{-1}(\boldsymbol{x}_0)WS(\boldsymbol{x}_0), \tag{57}$$

when $\boldsymbol{x}_{\text{final}} = \boldsymbol{x}_0$. Thus only the eigenvalues of W are gauge invariant.

1.8 Relation Between U_a and W

[Source handwritten page 10]

The notes compare the full projector-space adiabatic evolution with the Wilson line written in a basis.

Define

$$W_A(\gamma) = P(\boldsymbol{x}_\mathrm{f}) U_a(\gamma) P(\boldsymbol{x}_0). \tag{58}$$

This operator maps the initial occupied subspace to the final occupied subspace. The finite-dimensional matrix W is its representation in the chosen bases at the endpoints.

The notes state that W_A and W share the same nonzero spectral data for a closed loop. The operator expression obeys a differential equation of the form

$$\mathrm{d}W_A = [\mathrm{d}P, P] W_A, \qquad W_A(0) = P(0). \tag{59}$$

The basis Wilson line obeys

$$\mathrm{d}W = \mathrm{i}AW, \qquad W(0) = \mathbb{1}_N. \tag{60}$$

Transcription needed: The handwritten page contains a line comparing $W = PUP$ and the matrix W_{mn}, plus a phrase "same differential equation but different initial condition". The typed equations above capture the standard content, but the exact notation on the page should be checked.

1.9 Example: Electric Polarization

[Source handwritten page 10]

Consider Bloch eigenstates of a one-dimensional Hamiltonian:

$$H(k) \left| u_{n,k} \right\rangle = E_n(k) \left| u_{n,k} \right\rangle . \tag{61}$$

The full eigenstate has the Bloch form

$$\left| \psi_{n,k} \right\rangle = \mathrm{e}^{\mathrm{i}kx} \left| u_{n,k} \right\rangle . \tag{62}$$

[Source handwritten page 11]

Apply a small electric field E. In a gauge with vector potential

$$A(t) = Et, \tag{63}$$

minimal coupling gives

$$k \mapsto k + A(t). \tag{64}$$

For sufficiently slow variation, the adiabatic theorem applies and the cell-periodic part evolves according to a Wilson line:

$$\left| u_{n,k+A(t)} \right\rangle = \sum_m W_{mn}(t) \left| u_{m,k} \right\rangle . \tag{65}$$

The notes then consider the average many-body position. Let the many-body filled-band state be a Slater determinant built from occupied Bloch states:

$$\left| \Psi \right\rangle = \prod_{k \in \mathrm{BZ}} c_k^\dagger \left| 0 \right\rangle . \tag{66}$$

A many-body position operator can be written in exponentiated form,

$$\hat{X} = \exp\left(\frac{2\pi \mathrm{i}}{L}\sum_j x_j\right). \tag{67}$$

This operator is well defined under periodic boundary conditions.

Transcription needed: The handwritten derivation of the exponentiated position operator includes several OCR-corrupted creation/annihilation operator lines. The intended result is the Resta formula relating the expectation value of $\hat{X}$ to the many-body polarization.

[Source handwritten page 12]

Writing the many-body expectation value as a Slater determinant gives

$$\exp\left(\frac{2\pi \mathrm{i}}{e}P\right) = \langle\Psi|\,\hat{X}\,|\Psi\rangle = \det S, \tag{68}$$

where S is the overlap matrix between occupied states shifted by $2\pi/L$ in crystal momentum.

In the thermodynamic limit $L \to \infty$, the product of overlap matrices becomes the Wilson loop over the Brillouin zone:

$$\det S \longrightarrow \det W_{\mathrm{BZ}}. \tag{69}$$

Thus the gauge-invariant Wilson loop in the Brillouin zone is related to the mean center of charge:

$$P = \frac{e}{2\pi}\,\mathrm{Im}\log\det W_{\mathrm{BZ}} \pmod{e}. \tag{70}$$

2 Lecture 2: A Topological Insulator

2.1 Recap of Lecture 1

[Source handwritten page 13]

The first lecture introduced:

- adiabatic transport and geometric phase,
- a parameter manifold M,
- a family of Hamiltonians $H(\boldsymbol{x})$,
- a subspace of states $\mathcal{R}(\boldsymbol{x})$,
- a projector $P(\boldsymbol{x})$ onto that subspace,
- the adiabatic evolution operator U_a,
- the Berry connection A on a $U(N)$ bundle,
- gauge-invariant curvature $F = \mathrm{d}A + A \wedge A$ in the non-Abelian convention,
- Wilson loops and holonomies,
- electric polarization as
$$P = \operatorname{Im} \log \det W_{\mathrm{BZ}} \tag{71}$$
up to the physical prefactor $e/2\pi$.

The handwritten recap also says: instead of projectors one can use states, with

$$A_{mn} = \mathrm{i} \langle u_m \,|\, \mathrm{d}u_n \rangle \,, \tag{72}$$

and

$$W_{mn} = \langle u_m \,|\, U_a u_n \rangle \,. \tag{73}$$

2.2 Knowledge Assumed: Tight Binding and Bloch Theorem

[Source handwritten page 14]

The lecture assumes familiarity with tight-binding Hamiltonians and Bloch's theorem.

The single-particle Schrodinger equation in a periodic potential is

$$\left[\frac{\boldsymbol{p}^2}{2m} + V(\boldsymbol{r})\right] \psi_{n\boldsymbol{k}}(\boldsymbol{r}) = E_n(\boldsymbol{k}) \psi_{n\boldsymbol{k}}(\boldsymbol{r}). \tag{74}$$

Bloch's theorem states that solutions have the form

$$\psi_{n\boldsymbol{k}}(\boldsymbol{r}) = \mathrm{e}^{\mathrm{i}\boldsymbol{k}\cdot\boldsymbol{r}} u_{n\boldsymbol{k}}(\boldsymbol{r}), \tag{75}$$

where $u_{n\boldsymbol{k}}(\boldsymbol{r})$ is periodic in the lattice.

One can then work with the Bloch Hamiltonian

$$H(\boldsymbol{k}) \,|u_{n\boldsymbol{k}}\rangle = E_n(\boldsymbol{k}) \,|u_{n\boldsymbol{k}}\rangle \,. \tag{76}$$

In the tight-binding approximation, $H(\boldsymbol{k})$ becomes a finite matrix acting on orbital/sublattice degrees of freedom.

2.3 The Haldane Model

[Source handwritten page 14]

The Haldane model contains:

- nearest-neighbor hopping t_1,
- next-nearest-neighbor hopping amplitude t_2,
- Haldane phase ϕ,
- Semenoff mass M, i.e. staggered on-site energy.

The Hamiltonian is

$$H = t_1 \sum_{\langle i,j \rangle} c_i^\dagger c_j + t_2 \sum_{\langle\langle i,j \rangle\rangle} \mathrm{e}^{\mathrm{i}\nu_{ij}\phi} c_i^\dagger c_j + M \sum_i \xi_i c_i^\dagger c_i, \tag{77}$$

where $\nu_{ij} = \pm 1$ records the orientation of the next-nearest-neighbor hopping and $\xi_i = \pm 1$ on the two sublattices.

[Source handwritten page 15]

The Brillouin zone of the honeycomb lattice is compact and contains two inequivalent valleys K and K'.

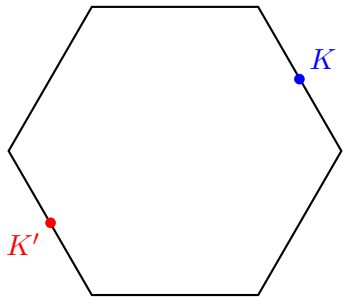

Schematic honeycomb Brillouin zone

Figure 2: Schematic Brillouin zone with inequivalent valleys.

The Bloch Hamiltonian can be written as

$$H(\boldsymbol{k}) = d_0(\boldsymbol{k}) \mathbb{1} + \boldsymbol{d}(\boldsymbol{k}) \cdot \boldsymbol{\sigma}. \tag{78}$$

The exact functions $d_0(\boldsymbol{k})$ and $\boldsymbol{d}(\boldsymbol{k})$ can be found in Bernevig and Hughes or derived from the honeycomb tight-binding model.

The two bands are

$$E_\pm(\boldsymbol{k}) = d_0(\boldsymbol{k}) \pm |\boldsymbol{d}(\boldsymbol{k})|. \tag{79}$$

The corresponding eigenvectors are not unique: each eigenstate has a local $U(1)$ gauge freedom

$$|u_\pm(\boldsymbol{k})\rangle \mapsto \mathrm{e}^{\mathrm{i}\phi_\pm(\boldsymbol{k})} |u_\pm(\boldsymbol{k})\rangle . \tag{80}$$

We are interested in the insulating phase, so the lower band is completely filled and forms the occupied subspace:

$$P(\boldsymbol{k}) = |u_-(\boldsymbol{k})\rangle \langle u_-(\boldsymbol{k})| . \tag{81}$$

2.4 Berryology of the Chern Insulator

[Source handwritten page 16]

The $U(1)$ Berry connection is

$$A_\mu(\boldsymbol{k}) = \mathrm{i}\left\langle u(\boldsymbol{k}) \,\middle|\, \partial_{k_\mu} u(\boldsymbol{k})\right\rangle. \tag{82}$$

It transforms under the $U(1)$ gauge transformation $|u\rangle \mapsto \mathrm{e}^{\mathrm{i}\phi}|u\rangle$ as

$$A_\mu \mapsto A_\mu - \partial_{k_\mu}\phi. \tag{83}$$

The gauge-invariant Berry curvature is

$$F_{\mu\nu} = \partial_\mu A_\nu - \partial_\nu A_\mu. \tag{84}$$

For a two-band model,

$$F_{xy} = \frac{1}{2}\hat{\boldsymbol{d}}\cdot\left(\partial_{k_x}\hat{\boldsymbol{d}}\times\partial_{k_y}\hat{\boldsymbol{d}}\right), \tag{85}$$

again up to a sign convention for upper versus lower band.

The first Chern number is

$$C = \frac{1}{2\pi}\int_{\mathrm{BZ}} F_{xy}\,\mathrm{d}k_x\,\mathrm{d}k_y. \tag{86}$$

2.5 Topological Interpretations

[Source handwritten page 16]

A. Map to the sphere. Consider the map

$$f: T^2 \to S^2, \qquad \boldsymbol{k} \mapsto \hat{\boldsymbol{d}}(\boldsymbol{k}). \tag{87}$$

The Jacobian of this map is twice the Berry curvature. The Chern number counts the number of times $\hat{\boldsymbol{d}}$ winds around the origin/sphere.

[Source handwritten page 17]

B. Algebraic-topology/differential-geometry picture. The name Chern comes from the fact that F is associated with the first Chern class, an element of the second cohomology class over integers:

$$c_1 \in H^2(T^2, \mathbb{Z}). \tag{88}$$

The curvature is locally $F = \mathrm{d}A$, but globally this need not imply a zero integral because A may not be globally defined. The Chern number is a topological invariant associated with the curvature of the connection on the $U(1)$ bundle.

C. Magnetic-monopole analogy. The notes compare Berry curvature with the magnetic field of a monopole. Gauss' law gives

$$\int_S \boldsymbol{B}\cdot\mathrm{d}\boldsymbol{S} = Q_B. \tag{89}$$

A nonzero integral of Berry curvature implies the presence of a monopole-like singularity in parameter space:

$$\int_S F \neq 0 \quad\Longleftrightarrow\quad \text{monopole enclosed.} \tag{90}$$

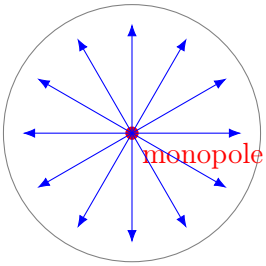

Curvature flux through a closed surface

Figure 3: Monopole analogy for nonzero Berry-curvature flux.

2.6 Physical Implication: Quantized Hall Conductance

[Source handwritten page 17]

The goal is to relate the Hall conductance of a two-dimensional system to the integral of Berry curvature:

$$\sigma_{xy} = \frac{e^2}{h}\frac{1}{2\pi}\int_{\mathrm{BZ}} F_{xy}\,\mathrm{d}^2k = \frac{e^2}{h}C. \tag{91}$$

[Source handwritten page 18]

Given a translationally invariant tight-binding Hamiltonian

$$H_0 = \sum_{ij,\alpha\beta} h_{ij}^{\alpha\beta} c_{i\alpha}^\dagger c_{j\beta}, \tag{92}$$

where i, j are spatial indices and α, β are internal indices, it couples to an external field by the Peierls substitution:

$$h_{ij}^{\alpha\beta} \mapsto h_{ij}^{\alpha\beta} \exp\left[\mathrm{i}e\int_{\boldsymbol{r}_i}^{\boldsymbol{r}_j} \boldsymbol{A}\cdot\mathrm{d}\boldsymbol{\ell}\right]. \tag{93}$$

Under reasonable approximations, expanding to first order in $\boldsymbol{A}$ gives

$$H = H_0 - \sum_{\boldsymbol{q}} j_i(\boldsymbol{q})A_i(-\boldsymbol{q}) + \cdots. \tag{94}$$

The current operator is the operator that couples linearly to the external field.

Linear-response theory gives the response of a many-body system in the ground state:

$$\langle j_i(\boldsymbol{q},\omega)\rangle = \sum_j R_{ij}(\boldsymbol{q},\omega)A_j(\boldsymbol{q},\omega), \tag{95}$$

where R_{ij} is a response kernel obtained from current-current correlation functions.

In Ohm's law,

$$j_i(\omega) = \sigma_{ij}(\omega)E_j(\omega), \tag{96}$$

and since

$$E_j(\omega) = \mathrm{i}\omega A_j(\omega), \tag{97}$$

one relates

$$\sigma_{ij}(\omega) = \frac{1}{\mathrm{i}\omega}R_{ij}(\omega). \tag{98}$$

[Source handwritten page 19]

The next steps require:

- the fluctuation-dissipation theorem,
- the relation between the response kernel and retarded Green's functions,
- computation of imaginary-time Green's functions,
- analytic continuation from Matsubara frequencies $\mathrm{i}\omega_n$ to real frequencies $\omega + \mathrm{i}0^+$.

The response kernel can be written schematically as

$$R_{ij}(\boldsymbol{q}, \mathrm{i}\omega_n) = \int_0^\beta \mathrm{d}\tau\, \mathrm{e}^{\mathrm{i}\omega_n \tau} \langle T_\tau j_i(\boldsymbol{q}, \tau) j_j(-\boldsymbol{q}, 0)\rangle. \tag{99}$$

After analytic continuation,

$$\sigma_{ij}(\omega) = \frac{1}{\mathrm{i}\omega} R_{ij}(\omega + \mathrm{i}0^+). \tag{100}$$

Performing an adiabatic transformation to the band basis yields a gauge-invariant formula. In the flat-band/occupied-band projector notation, the result can be expressed in terms of the occupied projector P_0:

$$\sigma_{xy} \propto \mathrm{Tr}\left[P_0[\partial_{k_x} P_0, \partial_{k_y} P_0]\right]. \tag{101}$$

Written in terms of Bloch states, this becomes

$$\sigma_{xy} = \frac{e^2}{h} \frac{1}{2\pi} \sum_{n \in \mathrm{occ}} \int_{\mathrm{BZ}} F_{xy}^{(n)}(\boldsymbol{k})\, \mathrm{d}^2 k. \tag{102}$$

For many bands this is the TKNN formula.

Transcription needed: The handwritten derivation contains several intermediate terms involving $R_{ij}(\boldsymbol{q}, \mathrm{i}\omega_m)$, traces over current operators, and band projectors. The exact line-by-line algebra is not fully legible, but the logical sequence FDT → imaginary-time Green's function → analytic continuation → projector/Berry-curvature formula is preserved here.

2.7 Chern-Simons Action

[Source handwritten page 20]

The Hall conductivity appears in the response

$$j_i = \sigma_H \epsilon_{ij} E_j. \tag{103}$$

The continuity equation and Maxwell relations can be written covariantly as

$$j^\mu = \sigma_H \epsilon^{\mu\nu\rho} \partial_\nu A_\rho. \tag{104}$$

Consider the Chern-Simons action for a background gauge field:

$$S_{\mathrm{CS}} = \frac{\sigma_H}{2} \int \mathrm{d}^3 x\, \epsilon^{\mu\nu\rho} A_\mu \partial_\nu A_\rho. \tag{105}$$

Varying with respect to the gauge field gives

$$j^\mu = \frac{\delta S_{\mathrm{CS}}}{\delta A_\mu} = \sigma_H \epsilon^{\mu\nu\rho} \partial_\nu A_\rho. \tag{106}$$

At the quantum level this coefficient is forced to be quantized. Under a gauge transformation

$$A_\mu \mapsto A_\mu + \partial_\mu f, \tag{107}$$

the action changes by a total derivative locally. When there is a global obstruction, the total derivative need not vanish. Requiring

$$\mathrm{e}^{\mathrm{i}S} \tag{108}$$

to be gauge invariant leads to quantization of the coefficient.

The notes indicate that integrating out fermions of a Chern insulator coupled to A_μ produces a Chern-Simons action in the low-energy effective theory.

Transcription needed: The handwritten Chern-Simons quantization argument contains Euclidean path-integral steps and a compact-gauge-transformation calculation. The exact factors of 2π and μ, ν, ρ indices should be checked against the scan.

3 Lecture 3: Topological Insulator Continued

3.1 Recap

[Source handwritten page 21]

The previous lectures established:

- adiabatic transport and geometric phase,
- Berry connection A and curvature F,
- the Haldane model for Chern insulators,
- occupied subspace described by a projector

$$P(\boldsymbol{k}) = |u_-(\boldsymbol{k})\rangle \langle u_-(\boldsymbol{k})| , \tag{109}$$

- $U(1)$ gauge symmetry of occupied states,
- Berry connection

$$A_\mu = \mathrm{i} \langle u \,|\, \partial_\mu u \rangle , \tag{110}$$

- Berry curvature

$$F_{xy} = \frac{1}{2} \hat{\boldsymbol{d}} \cdot \left(\partial_{k_x} \hat{\boldsymbol{d}} \times \partial_{k_y} \hat{\boldsymbol{d}} \right) . \tag{111}$$

[Source handwritten page 22]

The first Chern number is the integral of Berry curvature:

$$C = \frac{1}{2\pi} \int_{\mathrm{BZ}} F_{xy} \, \mathrm{d}^2 k. \tag{112}$$

Its interpretations:

1. C counts the winding of the map $\hat{\boldsymbol{d}} : T^2 \to S^2$.
2. F is the first Chern class in second cohomology over integers.
3. Nonzero curvature flux implies monopole-like singularities.

The quantized Hall conductance follows from the TKNN formula:

$$\sigma_{xy} = \frac{e^2}{h} C. \tag{113}$$

Equivalently, σ_{xy} is quantized to avoid a quantum anomaly of the Chern-Simons action:

$$S_{\mathrm{CS}} = \frac{k}{4\pi} \int A \wedge \mathrm{d}A. \tag{114}$$

3.2 Obstruction to Wannierization

[Source handwritten page 23]

The Brillouin zone has no boundary. Therefore a naive application of Stokes' theorem would say

$$\int_{\mathrm{BZ}} F = \int_{\mathrm{BZ}} \mathrm{d}A = \int_{\partial \mathrm{BZ}} A = 0. \tag{115}$$

This fails when the Berry connection A cannot be chosen smoothly over the entire Brillouin zone.

For two-dimensional Chern insulators, the obstruction is visible by covering the Brillouin zone with two patches. Let the Brillouin zone be split into regions R_1 and R_2, with smooth gauges chosen on each patch:

$$|u_1(\boldsymbol{k})\rangle = \mathrm{e}^{\mathrm{i}\phi(\boldsymbol{k})}\,|u_2(\boldsymbol{k})\rangle \quad \text{on } R_1 \cap R_2. \tag{116}$$

The Berry potentials satisfy

$$A_1 = A_2 - \mathrm{d}\phi. \tag{117}$$

Thus

$$\begin{aligned} 2\pi C &= \int_{\mathrm{BZ}} F && (118)\\ &= \int_{R_1} F + \int_{R_2} F && (119)\\ &= \int_{\partial R_1} A_1 + \int_{\partial R_2} A_2 && (120)\\ &= \oint_{\partial R_1} (A_1 - A_2) && (121)\\ &= -\oint_{\partial R_1} \mathrm{d}\phi. && (122) \end{aligned}$$

Single-valuedness of the wavefunction implies that the phase winding is an integer:

$$\oint \mathrm{d}\phi = 2\pi n, \tag{123}$$

so $C \in \mathbb{Z}$.

[Source handwritten page 24]

For a two-band model, one can see the obstruction explicitly from eigenvector choices on the sphere. A common lower-band spinor gauge is

$$|u_-(\theta,\phi)\rangle = \begin{pmatrix} -\mathrm{e}^{-\mathrm{i}\phi}\sin(\theta/2) \\ \cos(\theta/2) \end{pmatrix}. \tag{124}$$

This gauge is smooth at one pole but singular at the other. Another choice,

$$|u'_-(\theta,\phi)\rangle = \begin{pmatrix} -\sin(\theta/2) \\ \mathrm{e}^{\mathrm{i}\phi}\cos(\theta/2) \end{pmatrix}, \tag{125}$$

has the opposite singularity. The two are related by a gauge transformation on the overlap.

Transcription needed: The handwritten page shows two explicit spinor gauges and notes that at $\theta = 0$ or $\theta = \pi$ the same point in space is represented by multivalued phases. The exact spinor convention may differ by signs and which pole is singular.

[Source handwritten page 25]

Because a globally smooth gauge cannot be defined for a nonzero Chern band, one cannot define exponentially localized Wannier functions for that isolated band:

$$|w_R\rangle = \frac{1}{\sqrt{N}} \sum_k \mathrm{e}^{-\mathrm{i}kR} |\psi_k\rangle \,. \tag{126}$$

The obstruction is the topology of the Bloch bundle.

3.3 Determining a Topological Phase Transition from a Dirac Hamiltonian

[Source handwritten page 25]

A generic Dirac Hamiltonian can be written as

$$h(\boldsymbol{k}) = d_x(\boldsymbol{k})\sigma_x + d_y(\boldsymbol{k})\sigma_y + d_z(\boldsymbol{k})\sigma_z. \tag{127}$$

Near a gap closing,

$$d_x = t_{xx}k_x + t_{xy}k_y, \tag{128}$$
$$d_y = t_{yx}k_x + t_{yy}k_y, \tag{129}$$
$$d_z = M. \tag{130}$$

The mass term M opens the gap.

The Berry curvature integral for a massive Dirac point gives a half-quantized contribution:

$$\sigma_{xy}^{\mathrm{Dirac}} = \frac{1}{2} \operatorname{sgn}(M) \operatorname{sgn} \det(t), \tag{131}$$

in units of e^2/h, where

$$t = \begin{pmatrix} t_{xx} & t_{xy} \\ t_{yx} & t_{yy} \end{pmatrix}. \tag{132}$$

[Source handwritten page 26]

The notes indicate this follows by using identities for the two-band Berry curvature and integrating over the Dirac continuum. The result is half quantized because the continuum Dirac theory is blind to the lattice regularization. A lattice model lives on a compact manifold and supplies the other half through high-energy spectator fermions or band bending.

For the Haldane model, topological phase transitions occur at gap closings near the valleys K and K'. The low-energy Hamiltonians are Dirac Hamiltonians with valley-dependent masses. Schematically,

$$H_{K/K'}(\boldsymbol{q}) = v_x q_x \sigma_x + v_y q_y \sigma_y + m_{K/K'}\sigma_z, \tag{133}$$

with

$$m_{K/K'} = M \mp 3\sqrt{3}\, t_2 \sin\phi. \tag{134}$$

At large $|M|$, the system is a trivial insulator, essentially localized on the A or B sublattice:

$$\sigma_{xy} = 0. \tag{135}$$

At

$$M = \pm 3\sqrt{3}\, t_2 \sin\phi \tag{136}$$

the gap closes, and crossing this line changes the Chern number by one.

[Source handwritten page 27]

The phase diagram is:

$$\begin{cases} C = 0, & |M| > 3\sqrt{3}|t_2 \sin\phi|, \\ C = \operatorname{sgn}(\sin\phi), & |M| < 3\sqrt{3}|t_2 \sin\phi|, \end{cases} \tag{137}$$

up to sign conventions.

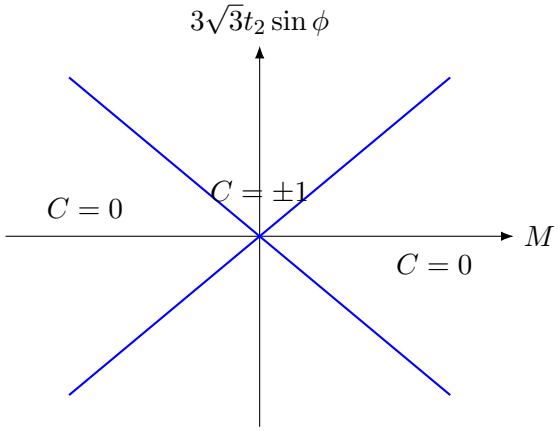

Schematic Haldane phase diagram

Figure 4: Topological and trivial regions separated by Dirac gap closings.

3.4 Gapless Chiral Edge Modes

[Source handwritten page 27]

Consider two infinite samples with an interface along the y direction. The Hall conductance differs across the interface:

$$\sigma_{xy}^{\text{left}} \neq \sigma_{xy}^{\text{right}}. \tag{138}$$

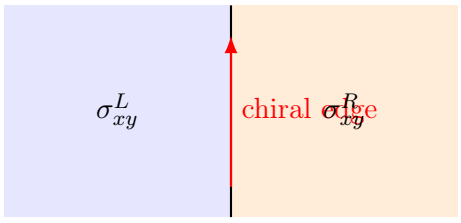

Interface parallel to y

Figure 5: Domain wall between two insulating regions.

Since the mass term is responsible for the topological phase transition, model the interface by a spatially varying mass $m(x)$ such that

$$m(x \to -\infty) < 0, \qquad m(x \to +\infty) > 0, \tag{139}$$

or vice versa.

[Source handwritten page 28]

The continuum Hamiltonian is

$$H = -\mathrm{i}\sigma_x\partial_x - \mathrm{i}\sigma_y\partial_y + m(x)\sigma_z. \tag{140}$$

Use the ansatz

$$\psi(x,y) = \mathrm{e}^{\mathrm{i}k_y y}\phi(x), \tag{141}$$

where $\phi(x)$ is a two-component spinor. Then

$$E\phi = \left[-\mathrm{i}\sigma_x\partial_x + k_y\sigma_y + m(x)\sigma_z\right]\phi. \tag{142}$$

At $E = 0$ and $k_y = 0$, impose

$$\sigma_y\phi = \lambda\phi \tag{143}$$

or an equivalent spinor constraint, depending on the chosen Pauli-matrix convention. Then the equation reduces to

$$\partial_x\phi(x) = -m(x)\phi(x) \tag{144}$$

up to a sign fixed by the normalizable solution.

The solution is

$$\phi(x) = \exp\left[-\int_0^x m(x')\,\mathrm{d}x'\right]\chi, \tag{145}$$

where χ is the spinor satisfying the constraint. Normalizability selects one chirality. Including finite k_y gives

$$E(k_y) = vk_y \tag{146}$$

with a sign determined by the mass-domain-wall orientation.

Thus:

1. the state is localized at the domain wall;
2. the propagation along y is chiral.

Transcription needed: The handwritten spinor constraint is OCR-corrupted as "$i\sigma_x \ldots$". The typed derivation gives the standard Jackiw-Rebbi edge-mode result, but the exact Pauli-matrix convention should be checked.

3.5 The Role of Symmetry

[Source handwritten page 29]

Starting from the graphene semimetal, one can see that breaking different symmetries opens different types of gaps.

The graphene tight-binding Hamiltonian has the form

$$H(\boldsymbol{k}) = \begin{pmatrix} 0 & f(\boldsymbol{k}) \\ f^*(\boldsymbol{k}) & 0 \end{pmatrix} = d_x(\boldsymbol{k})\sigma_x + d_y(\boldsymbol{k})\sigma_y. \tag{147}$$

The off-diagonal function is

$$f(\boldsymbol{k}) = t\sum_{j=1}^{3}\mathrm{e}^{\mathrm{i}\boldsymbol{k}\cdot\boldsymbol{\delta}_j}. \tag{148}$$

There are two Dirac cones at K and K'. Near them,

$$H_K(\boldsymbol{q}) = v(q_x\sigma_x + q_y\sigma_y), \tag{149}$$

and

$$H_{K'}(\boldsymbol{q}) = v(-q_x\sigma_x + q_y\sigma_y), \tag{150}$$

up to convention. The two valleys are time-reversal partners:

$$K \leftrightarrow K'. \tag{151}$$

A. Inversion Symmetry

Inversion exchanges the sublattices A and B:

$$\mathcal{I}c_{i,A}\mathcal{I}^{-1} = c_{-i,B}, \qquad \mathcal{I}c_{i,B}\mathcal{I}^{-1} = c_{-i,A}. \tag{152}$$

In momentum space it imposes

$$\mathcal{I}H(\boldsymbol{k})\mathcal{I}^{-1} = H(-\boldsymbol{k}). \tag{153}$$

For the sublattice basis, inversion is represented by σ_x up to a choice of origin:

$$\mathcal{I} \sim \sigma_x. \tag{154}$$

[Source handwritten page 30]

B. Time-Reversal Symmetry

For spinless fermions,

$$\mathcal{T} = \mathcal{K}, \qquad \mathcal{T}^2 = 1, \tag{155}$$

where $\mathcal{K}$ denotes complex conjugation. Time reversal imposes

$$H(\boldsymbol{k}) = H^*(-\boldsymbol{k}). \tag{156}$$

The notes emphasize that a single Dirac cone is not protected by time reversal or inversion separately. Different symmetry-breaking masses are possible:

- **Inversion breaking, time-reversal preserving:** a Semenoff mass

  $$H_M = M\sigma_z \tag{157}$$

  opens a sublattice gap. This is topologically trivial.

- **Time-reversal breaking, inversion preserving:** a Haldane mass changes sign between valleys:

  $$H_K = v(q_x\sigma_x + q_y\sigma_y) + m\sigma_z, \tag{158}$$

  $$H_{K'} = v(-q_x\sigma_x + q_y\sigma_y) - m\sigma_z. \tag{159}$$

  This yields a Chern-insulating phase.

Stability of Dirac Nodes

If both inversion and time-reversal symmetry are present, no σ_z mass term is allowed locally. The Dirac cones are protected by the combined symmetry. Each valley carries a vorticity, equivalently a Berry phase of π:

$$\gamma = \oint A = \pi \pmod{2\pi}. \tag{160}$$

If perturbations are large enough, Dirac cones with opposite vorticity can meet and annihilate.

[Source handwritten page 31]

The final handwritten note says that the symmetry actually fixes the Dirac points, giving a form of global stability:

$$\mathcal{IT} \quad \text{forces Dirac points to be fixed.} \tag{161}$$

Transcription needed: The final page is a short statement about global stability under combined inversion-time-reversal symmetry. The exact wording is OCR-read as "sym actually ITCs forces Dirac points to be fixed Global stability".